Environmental Science

Volume 2, Issue 3, 607-622.
DOI: 10.3934/environsci.2015.3.607
Received date 6 May 2015,
Accepted date 17 June 2015,
Published date 23 June2015

http://www.aimspress.com/

Research article

Revisiting spontaneous silver nanoparticles formation: a factor influencing the determination of minimum inhibitory concentration values?

Karolína M. Šišková [1,*], Renáta Večeřová [2], Hana Kubičková [1], Magdaléna Bryksová [1], Klára Čépe [1] and Milan Kolář [2]

[1] Faculty of Science, Palacký University in Olomouc, Šlechtitelů 11, 78371 Olomouc, Czech Republic
[2] Department of Microbiology, Faculty of Medicine and Dentistry, Palacký University in Olomouc, Hněvotínská 3, 77146 Olomouc, Czech Republic

* **Correspondence:** karolina.siskova@upol.cz; Tel: + 420-585-634-955; Fax: + 420-585-634-958.

Abstract: The present study gives evidence that silver nanoparticles (AgNPs) are spontaneously formed from Ag^+ ions in Mueller-Hinton broth, which is frequently used as a standard cultivation medium for many types of bacteria. Silver ions often serve as a reference in the determination of minimum inhibitory concentration (MIC) values of engineered AgNPs. It is thus a question if the MIC values determined for engineered AgNPs are not influenced by the presence of spontaneously formed AgNPs. Furthermore, as shown here, the addition of augmented concentrations of selected amino acids, namely glutamic acid and glutamine, can change the growth and characteristic features of spontaneously formed AgNPs. For the sake of a direct comparison, the influence of the two selected amino acids on characteristics and MIC values determination of engineered AgNPs has been also investigated. The determined MIC values of all investigated systems (i.e., with and without the presence of engineered AgNPs) and their mutual comparison demonstrated that MIC values are slightly influenced by the actual composition of a cultivation medium for bacterial growth. On the other hand, the actual composition of a cultivation medium is crucial for the final characteristics of AgNPs. The changes in characteristic features of spontaneously formed as well as engineered AgNPs are most probably induced by the covalent bonding of amino acids to AgNPs surface which is proven by vibrational spectroscopic techniques.

Keywords: Ag nanoparticle; glutamic acid; glutamine; Mueller–Hinton medium; antibacterial activity; antimicrobial test; covalent bond; surface-enhanced Raman spectroscopy

1. Introduction

There are persistent rumors about nanoparticles toxicity and ecotoxicity, concerns about their increasing release into the environment and attempts of their risk assessment [1–5]. Silver nanoparticles (AgNPs) among others (like for example titanium dioxide) belong to the most frequently used ones due to their unique optical, catalytic, sensing and antimicrobial properties. They are declared to be present in consumer products such as cloths and textiles, tooth brushes and pastes, cosmetics, mobile phones and so forth [6,7]. It has been also evidenced in the literature that AgNPs can be spontaneously formed under environmentally relevant conditions [8–10]. Thus, there are not only engineered AgNPs which can circulate in the environment.

Antimicrobial properties of AgNPs are often tested employing a standard microdilution method [11] which results in minimum inhibitory concentration (MIC) value determination. Mueller-Hinton broth (M-H Broth) is a standard cultivation medium for many types of bacteria as recommended by Clinical and Laboratory Standards Institute (CLSI), Food and Drug Administration (FDA), European Committee on Antimicrobial Susceptibility Testing (EUCAST), and World Health Organization (WHO) [12]. It comprises amino acids, vitamins, nitrogenous compounds (all three types of compounds stemming from beef infusion), starch and a lot of casein hydrolysate (consisting of proteins rich in oligopeptides). The final pH is 7.4 ± 0.2 at 25 ℃ [12]. Many of the compounds which are present in M-H Broth can create AgNPs, even though used separately as evidenced in the literature [13–29], by reducing Ag^+ under certain conditions (e.g. alkaline pH, slightly increased temperature etc.). Indeed, there are several papers dealing with AgNPs generation induced by amino acids in alkaline media [17–21], vitamins [22,23], nitrogenous compounds [24,25], proteins [26], polyaminoacids [27], sacharides [28], and starch [29]. Starch, peptides, polyaminoacids and nitrogenous compounds can also serve as good biocompatible capping agents of AgNPs [29–33]. Therefore, there is a real chance that AgNPs are spontaneously formed from Ag^+ ions in M-H Broth. In the present work, we test this hypothesis which has never been addressed so far. It is of an utmost importance especially when the antibacterial activity of various types of AgNPs is determined and MIC values compared with that of $AgNO_3$ solution serving usually as a reference.

Silver ions and AgNPs are both well known and used as efficient antibacterial agents [34–37]. It is generally accepted that Ag^+ and AgNPs are effective at many bacterial cell levels: they are able to inactivate bacterial enzymes [37,38], disrupt bacterial metabolic processes [39–41] and the bacterial cell wall, accumulate in the cytoplasmic membrane and increase its permeability [37,42,43], interact with DNA [38] and generate reactive oxygen species [44,45]. One of the important target sites is the bacterial cell wall which is significantly different in Gram-positive as compared with Gram-negative bacteria. We have thus tested two bacterial strains of both types in the present study, namely: Staphylococcus aureus CCM 3953 (Gram-positive), Staphylococcus epidermidis 879 (Gram-positive), Pseudomonas aeruginosa CCM 3955 (Gram-negative), Klebsiella pneumoniae (ESBL-positive strain) (Gram-negative).

Recent paper of Zong-ming Xiu and coworkers [46] has given clear evidence that Ag^+ release from AgNPs is the main factor causing AgNPs toxicity. The Ag^+ release is highly influenced by

aerobic conditions, size, shape, and coating of AgNPs [46]. Furthermore, it can be declared that AgNPs coating strongly affects their zeta potential values [33,47]. Surface properties of bacteria species (negative or positive charging) can then come into play as well and result into either favorable, or unfavorable particle-cell electrostatic interactions [35]. Moreover, a study dealing with charge-dependent transport and toxicity of peptide-functionalized AgNPs has been published recently [33]. The authors [33] have demonstrated by the tests using zebrafish embryos that AgNPs with positive zeta potential values are less toxic than those possessing negative values. The peptides employed have differed in a single amino acid at its C-terminus [33]. The most toxic peptide in their work [33] has been ended by L-glutamic acid. For this reason, in the present work we have focused our attention on the influence of L-glutamic acid (E) as a direct surface-modifier of AgNPs. For the sake of comparison, glutamine (Q) in augmented concentrations has been also selected. It is demonstrated that the addition of these two amino acids can change zeta potential values and the other characteristics of engineered as well as spontaneously formed AgNPs.

Characteristic features of AgNPs were determined by transmission electron microscopy (TEM), dynamic light scattering (DLS), zeta potential values measurements, and UV-Vis absorption spectroscopy in the present study. Surface modification of AgNPs by the two selected amino acids was investigated by the methods of vibrational spectroscopy, namely, infrared (IR) absorption and surface-enhanced Raman scattering (SERS).

2. Materials and Method

2.1. Chemicals

Silver nitrate (> 99.0% purity, $AgNO_3$) purchased from Lachema (Czech Republic) was not purified prior to its use. Sodium borohydride ($NaBH_4$) purchased from Sigma-Aldrich, stored under humidity-limited conditions (no longer than for half year) was employed. L-glutamic acid (E) and L-glutamine (Q) provided by Sigma-Aldrich were stored under laboratory conditions and used as received. Mueller-Hinton broth (M-H Broth) was purchased from Difco (Becton, Dickinson and Company). All glassware including spectroscopic cuvettes were washed with diluted (1:1 v/v) nitric acid (Penta, Czech Republic) and several times thoroughly rinsed with deionized water.

2.2. Spontaneous formation of AgNPs in M-H Broth

2.35×10^{-4} M of $AgNO_3$ was prepared and used as a stock solution for all systems. Then, 3 mL of $AgNO_3$ stock solution and 3 mL of M-H Broth were mixed together in a testing tube, stored in dark at 37 ℃ for 24 hours. Characterization by DLS, TEM, UV-Vis was then performed. In the case of systems containing E and/or Q, the system preparations included the addition of E/Q into $AgNO_3$ solution, the molar ratio between Ag^+ and AA was hold 1:1 and 1:10.

2.3. Synthesis of borohydride-reduced Ag colloid (Agbh)

Engineered AgNPs were prepared in exactly the same way as described in details in ref. [48]: an aqueous solution (9 mL) of 2.2×10^{-3} M $AgNO_3$ was added drop-wise into 75 mL of 1.1×10^{-3} M aqueous solution of $NaBH_4$ stirred in an Erlenmayer flask placed in an ice-bath. The ice-bath was

removed five minutes after the addition of the last drop of silver nitrate solution. Stirring was continued for another 45 min to adjust the Ag colloid to laboratory temperature. Then, 10 min of heating at 40 ℃ was applied to the Ag colloid while stirring in order to facilitate oxidation of any non-reacted borohydride. Finally, the Ag colloid was allowed to cool down to laboratory temperature with continuous stirring. The resulting Ag colloid was yellow in color, with the maximum of surface plasmon extinction at 390 nm, containing particles of approximately 12 nm in diameter. It was stable for at least 3 months without addition of any stabilizers if stored in dark at room temperature.

2.4. Instrumentation

Transmission electron microscopic images were recorded on a JEOL JEM-2010 TEM. Dynamic light scattering (DLS) and zeta potential values were measured on a Zetasizer Nano Series (Malvern Instruments). UV-Vis spectra were collected on a Specord S600 (Analytic Jena) spectrophotometer by using 1 cm optical path length cuvettes at room temperature. Surface-enhanced Raman scattering (SERS) spectra were recorded on a DXR Raman microscope (Nicolet, Czech Republic) in backscattering mode, using macro-sampler for a 1 cm cuvette, employing the 633 nm excitation wavelength (of a He-Ne gas laser), 8 mW on the sample, 50 μm slit, 4× objective, and high resolution grating (3 cm^{-1} spectral resolution). Each SERS spectrum was accumulated 100 times for 1 s, baseline corrected in Omnic software and presented without any further smoothing. Infrared (IR) absorption spectra were measured on an iS5 IR spectrophotometer (Nicolet, Czech Republic) using attenuated total reflection (ATR) mode on ZnSe crystal, 64 scans, 2 cm^{-1} resolution. The IR absorption spectra were treated in Omnic software by the following procedures: subtraction of a background measured immediately before the collection of a sample spectrum, transformation from reflectance to absorbance, baseline correction, and transformation from absorbance to transmittance.

2.5. Antibacterial tests

Antimicrobial activities of the systems were investigated using a standard microdilution method, which has been described in details elsewhere [11]. Minimum inhibitory concentration (MIC) values of AgNPs inducing the inhibition of bacterial growth are determined by this method. The antimicrobial tests were carried out in disposable microtitration plates and repeated three times in duplicates. Four bacterial strains were tested: Staphylococcus aureus CCM 3953 (Czech Collection of Microorganisms, Masaryk University in Brno, Czech Republic), Staphylococcus epidermidis 879 (isolated from the clinical material of a patient of the University Hospital in Olomouc, Czech Republic), Pseudomonas aeruginosa CCM 3955 (Czech Collection of Microorganisms, Masaryk University in Brno, Czech Republic), Klebsiella pneumoniae ESBL-positive strain (isolated from the clinical material of a patient of the University Hospital in Olomouc, Czech Republic).

3. Results and Discussion

3.1. Evidence of spontaneous AgNPs formation from $AgNO_3$ in M-H Broth

Standard microdilution method for the determination of MIC values [11] was performed for $AgNO_3$ solution and AgNPs prepared by borohydride-induced chemical reduction (Agbh). Both

solutions contained the same initial concentration of Ag^+, i.e. 2.35 $\times 10^{-4}$ M. During the antibacterial tests, we observed changes in color for the samples containing $AgNO_3$ and M-H Broth after 24 hours of incubation with a microbe, while almost no color changes were observed for Agbh under the same experimental conditions—Figure 1.

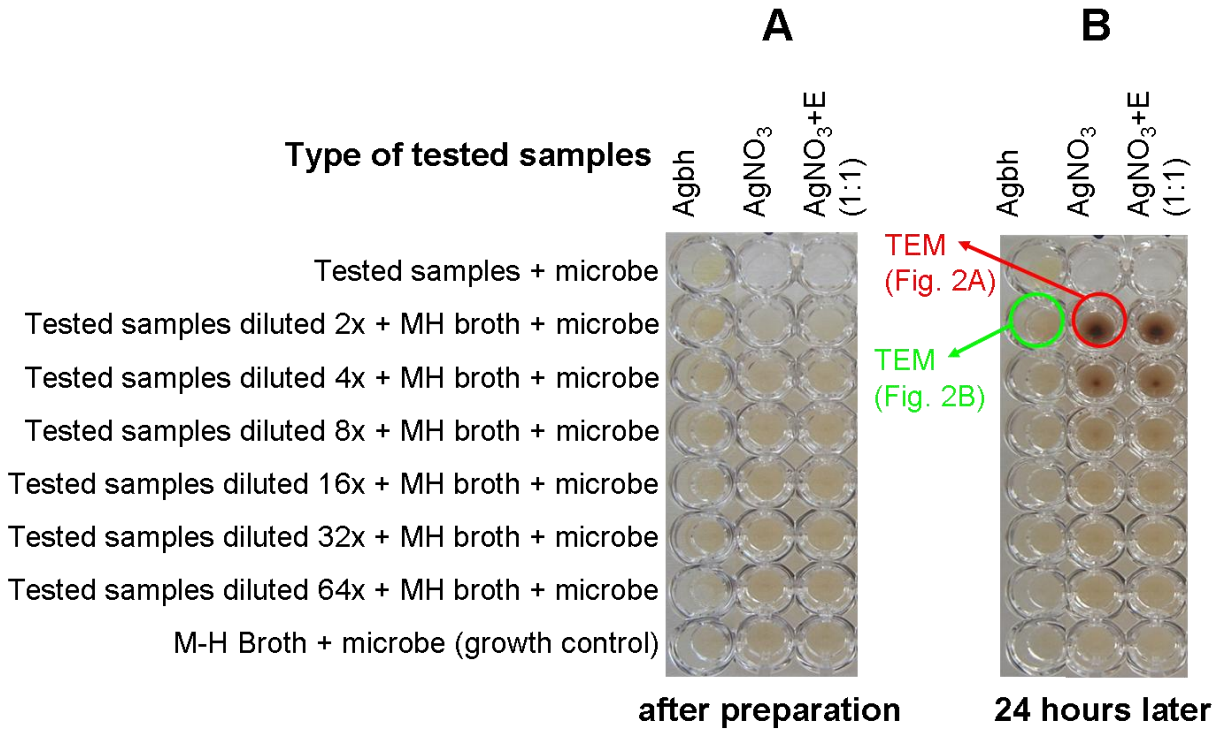

Figure 1. Evidence for deep color change of the samples containing $AgNO_3$ and/or $AgNO_3$ +E (molar ratio being 1:1), M-H Broth and a microbe (Staphylococcus epidermidis 879) when photos taken (A) immediately and (B) after 24 hours of incubation at 37 ℃ in dark. For the sake of a direct comparison, a sample containing Agbh which was tested under the same conditions is also shown. Wells which TEM images were recorded from are marked.

Considering the composition of M-H Broth (amino acids, vitamins, nitrogenous compounds, starch, oligopeptides) [12], the conditions of microbes cultivation [11] and taking into account the results published and discussed in the literature [13–29], we hypothesized that AgNPs could be formed and aggregated as obvious namely from the wells in the second column, the second and third lines in Figure 1B. Therefore, a small amount of the sample (in the second column and the second line in Figure 1B) was taken, deposited on a TEM grid, allowed to dry and measured. The microscopic image presented in Figure 2A then confirmed our working hypothesis about spontaneous AgNPs formation in M-H Broth under microbe cultivation conditions. The sample seemed to contain bigger (above 50 nm) and small (below 10 nm) particles, thus a bimodal size distribution (Figure 2A).

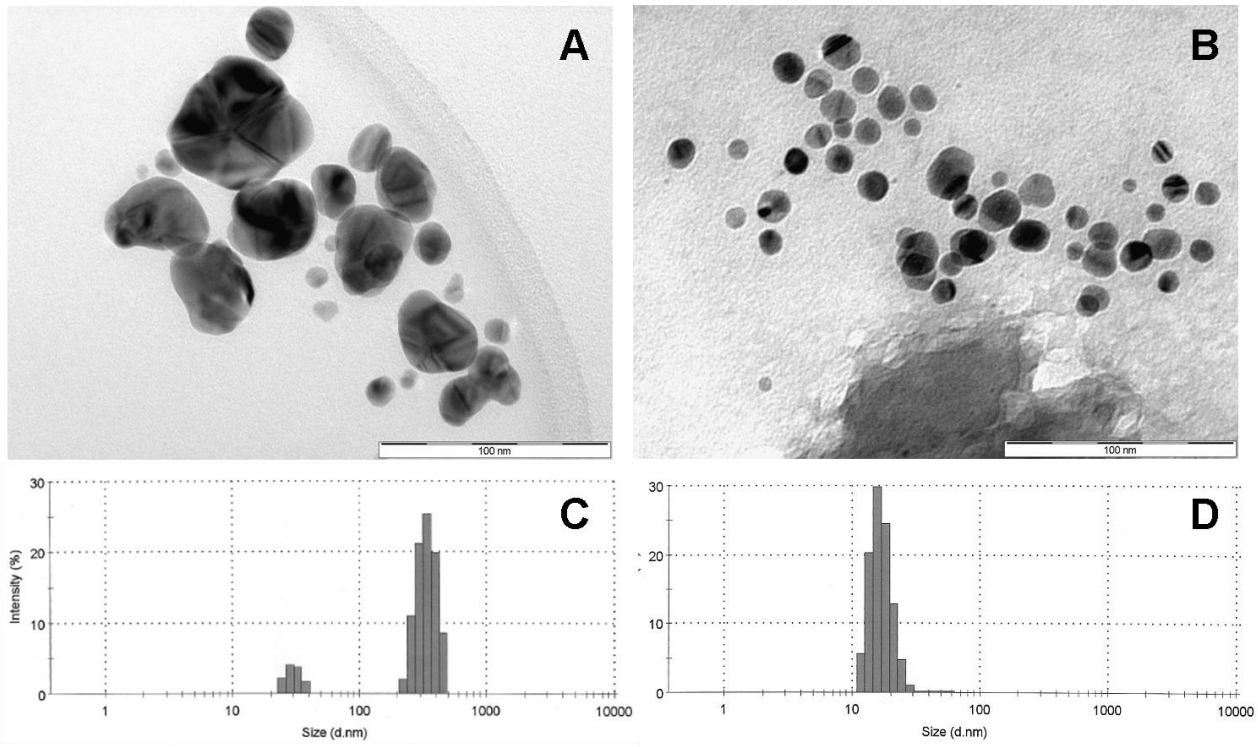

Figure 2. TEM images of AgNPs (A) spontaneously formed from $AgNO_3$ in M-H Broth+microbe medium, while (B) engineered Agbh in M-H Broth+microbe medium. Histograms of intensity-based particle size distribution determined by DLS in solutions of (C) $AgNO_3$+M-H Broth and (D) Agbh+M-H Broth.

For the sake of excluding any influence of the TEM sample preparation (drying etc.) on AgNPs formation, we also measured the microscopic images of the sample containing Agbh (engineered NPs) and M-H Broth and a microbe (thus the sample in the first column and the second line in Figure 1B)—TEM image shown in Figure 2B. It should be reminded that Agbh is known to contain almost monodispersed AgNPs of the average size of 10–12 nm in diameter [49,50]. It is thus quite obvious that AgNPs of Agbh remained of the same size as determined before any antibacterial testing and only aggregation was observed.

Dynamic light scattering was also employed in order to check the mean particle size in solutions of (i) $AgNO_3$+M-H Broth and (ii) Agbh+M-H Broth, after 24 h of their "cultivation" at 37 °C without any microbe in regular laboratory testing tubes (as described in section 2.2). This experiment was performed in order to exclude the possibility of AgNPs formation due to microplates and/or due to electron beam in TEM. The resulting histograms based on light intensity measurements are shown in Figure 2C–D. They revealed bimodal particle size distribution (PSD) for $AgNO_3$+M-H Broth (Figure 2C) and virtually monodispersed nanoparticles solution in the case of Agbh+M-H Broth (Figure 2D), thus similarly as derived from TEM images (Figure 2A–B). While particles of approximately 340 nm in diameter (88%) and nanoparticles of 30 nm in diameter (12%) could be encountered in the PSD in Figure 2C (i.e., $AgNO_3$+M-H Broth); nanoparticles of sizes around 17 nm in diameter (99%) dominated the PSD in Figure 2D (i.e., Agbh+M-H Broth). The mean particle sizes determined by TEM and DLS for a particular sample differ due to the well known fact that a contour of metallic particle is observed and visualized by TEM, whereas hydrodynamic diameter including

organic envelope and coating around each nanoparticle is determined by DLS measurements. Furthermore, intensity-based PSD of DLS measurements is the only one PSD determined purely experimentally (in comparison to number-based and/or volume-based PSDs), thus without any presumptions about e.g. shape of nanoparticles. On the other hand, intensity-based PSD is strongly influenced by the physical phenomenon that big particles scatter more light than the small ones resulting thus in a seemingly higher percentage of bigger particles. Therefore, the mutual counts of big vs. small particles within a sample have to be considered with a special care.

Another characteristic feature of AgNPs, surface plasmon extinction (SPE) band (extinction = absorption + scattering), was also determined for the above mentioned samples—Figure 3. The solution of $AgNO_3$+M-H Broth manifested itself by a very broad SPE band with the maximum positioned at around 463 nm and a small shoulder at around 350 nm (black curve in Figure 3A). This shape of SPE band well correlates with the presence of bigger and small particles of different morphologies as determined by DLS measurements and TEM images, respectively. On the contrary, Agbh revealed a narrow SPE band located at ~ 390 nm (black curve in Figure 3B) [48–50]. It should be pointed out that the SPE band of $AgNO_3$+M-H Broth (black curve in Figure 3A) is of a relatively low intensity in comparison to Agbh (black curve in Figure 3B) while the initial concentration of Ag^+ is the same (2.35×10^4 M) in both cases. This means, in turn, that the efficiency of AgNPs formation in M-H Broth is low (under standard microbe cultivation conditions) and not all $AgNO_3$ is transformed into AgNPs as confirmed by the presence of a shoulder positioned at 303 nm (black curve in Figure 3A). For the sake of a direct comparison, UV-Vis absorption spectrum of $AgNO_3$ solution in the employed concentration is also shown in Figure 3B.

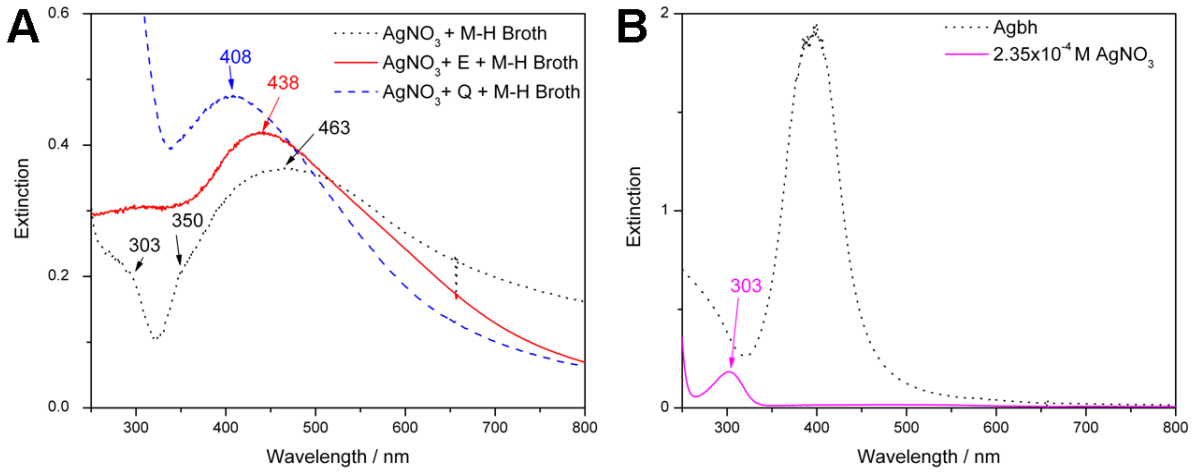

Figure 3. UV-Vis spectra of (A) $AgNO_3$+M-H Broth solutions incubated for 24 h: without (black dotted curve) and with glutamic acid (E, red solid curve, molar ratio of Ag^+:E is 1:1) and/or glutamine (Q, blue dashed curve, molar ratio of Ag^+:E is 1:1); (B) Agbh colloid (black dotted curve) and $AgNO_3$ solution (magenta solid curve).

Antibacterial testing of the $AgNO_3$ and Agbh solutions against two selected Gram-positive and Gram-negative bacterial strains (Figure 4) systematically revealed lower MIC values for $AgNO_3$ than

for Agbh (i.e., more toxic $AgNO_3$ than Agbh). It is in a good agreement with the literature [34] where the authors review and summarize the MIC values of AgNPs vs. $AgNO_3$ against various types of bacteria (in their Table 3), including bacteria which were tested in the present work. The MIC values of $AgNO_3$ are always approximately one order of magnitude lower than those of AgNPs of sizes 6–90 nm [34]. Why is it so? Although we have evidenced that AgNPs are formed in the system of M-H Broth+$AgNO_3$, we have also stated above that a remarkable portion of $AgNO_3$ remained in this system after 24 h. Taking into account the fact that a microbe is introduced, allowed to grow for 24 h and then the test is finished, the concentration of Ag^+ in the system of $AgNO_3$+M-H Broth is much higher during the testing period than that being obtained by a partial dissolution of AgNPs in the system of Agbh+M-H Broth. This results in a lower MIC value of $AgNO_3$ in comparison to Agbh although AgNPs are present in both systems.

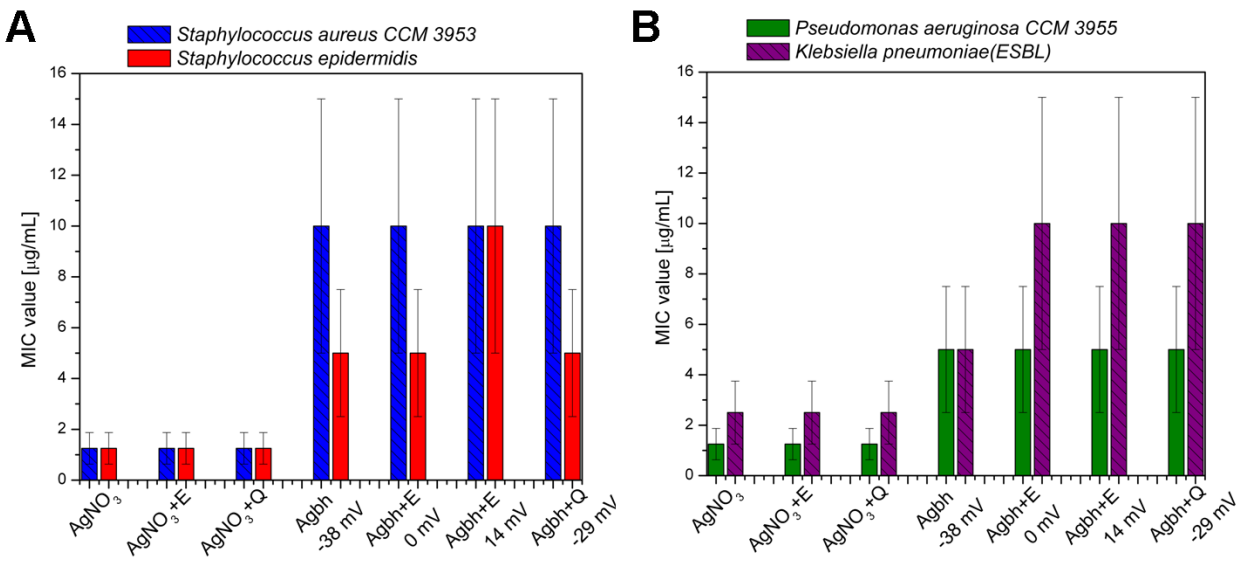

Figure 4. MIC values (y axis) of tested solutions (x axis) against two selected (A) Gram-positive and (B) Gram-negative bacterial strains whose names are specified above graphs. Experimental errors of MIC values determination for tested solutions are shown.

3.2. Influence of augmented concentrations of glutamic acid and/or glutamine on spontaneously formed AgNPs from $AgNO_3$ in M-H Broth

Since elevated concentrations of amino acids are known to increase the growth of bacteria [51], we started to be interested in the impact of two selected amino acids (E, Q) on AgNPs formed spontaneously in M-H Broth. E and Q were intentionally selected with respect to the results published in [33] and for the sake of a direct comparison, respectively. We assume that these two amino acids may potentially change the growth mechanism of AgNPs in the same M-H Broth used for the tests as in section 1 because they are supposed to interact with AgNPs surfaces by their amino- and carboxylic functional groups. Therefore, such experiments were carried out where the E and/or Q concentrations were adjusted to give the final molar ratio of 1:10 of Ag^+:AA.

UV-Vis spectra of the systems $AgNO_3$ +E/Q+M-H Broth, shown already in Figure 3A (for the sake of a direct comparison with the system of $AgNO_3$+M-H Broth, i.e., without any addition of

these two amino acids), revealed narrower SPE bands with the maxima being blue-shifted in comparison to the system of $AgNO_3$+M-H Broth: $AgNO_3$+E+M-H Broth possesses the maximum at 438 nm, whereas $AgNO_3$+Q+M-H Broth manifested itself by the maximum at 408 nm.

Visualization of spontaneously formed AgNPs by TEM images and determination of PSD by DLS measurements of $AgNO_3$+E/Q+M-H Broth (Figure 5) gave evidence about AgNPs formation with significantly different sizes than those presented in Figure 2A and C (i.e., $AgNO_3$+M-H Broth). Due to the presence of an increased E concentration, a bimodal size distribution of AgNPs remained (Figure 5C), but the histograms representing two size fractions are much closer to each other than in the case of $AgNO_3$+M-H Broth (Figure 2C). This is in agreement with morphologies and sizes of AgNPs being mostly encountered in TEM images (Figure 5A). The increased Q concentration also induced big changes in morphologies and sizes of AgNPs: a trimodal PSD was determined by DLS (Figure 5D) and confirmed by TEM imaging (Figure 5B).

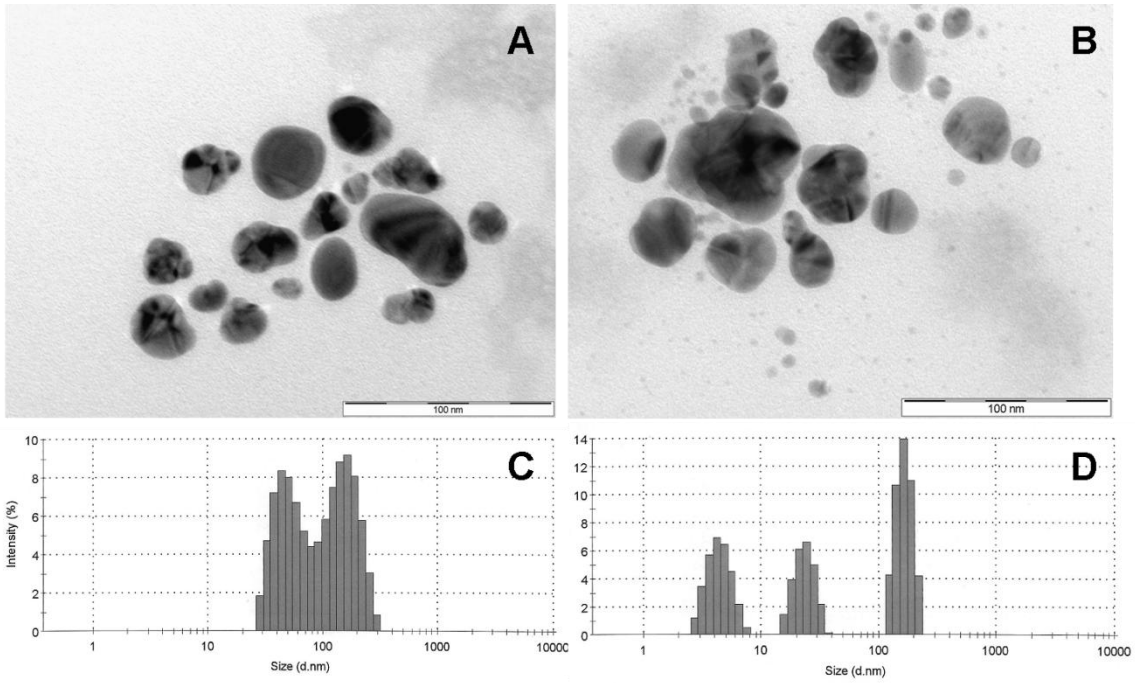

Figure 5. TEM images of AgNPs spontaneously formed from $AgNO_3$ in M-H Broth + microbe medium when (A) glutamic acid and/or (B) glutamine were present (Ag^+:AA ratio of 1:1). Histograms of intensity-based particle size distribution determined by DLS in solutions of (C) $AgNO_3$+E+M-H Broth, (D) $AgNO_3$+Q+M-H Broth.

Antibacterial tests were performed for these solutions containing $AgNO_3$+E/Q mixed together with M-H Broth as a cultivation medium. The resulting MIC values (Figure 4) were the same, for both of them, as that of the solution containing solely $AgNO_3$ and M-H Broth. It means that the increased concentrations of the two selected amino acids did not change MIC values. This gave again indirect evidence that the mode of antibacterial action in the systems containing spontaneously formed AgNPs in M-H Broth lies in the initial Ag^+ concentration rather than in spontaneously formed AgNPs presence although we can definitely change the growth and consequently characteristic features of these AgNPs by the addition of the increased concentrations of selected

amino acids into the cultivation medium. It can be thus summarized that the actual composition of M-H Broth has a tremendous impact on the shape, size, and aggregation state of the spontaneously formed AgNPs.

3.3. Engineered AgNPs (Agbh) surface-modified by glutamic acid and/or glutamine

Taking into account the results of the previous section, the interaction between E and/or Q and engineered AgNPs was tested. Two concentrations of amino acids were employed in order to get the final molar ratios between Ag and amino acid (Ag:AA) of 1:10 and 1:70. First of all, characteristic features of particular colloidal systems were measured, such as UV-Vis spectra, zeta potential values (Figure 6) and AgNPs mean sizes determined by DLS.

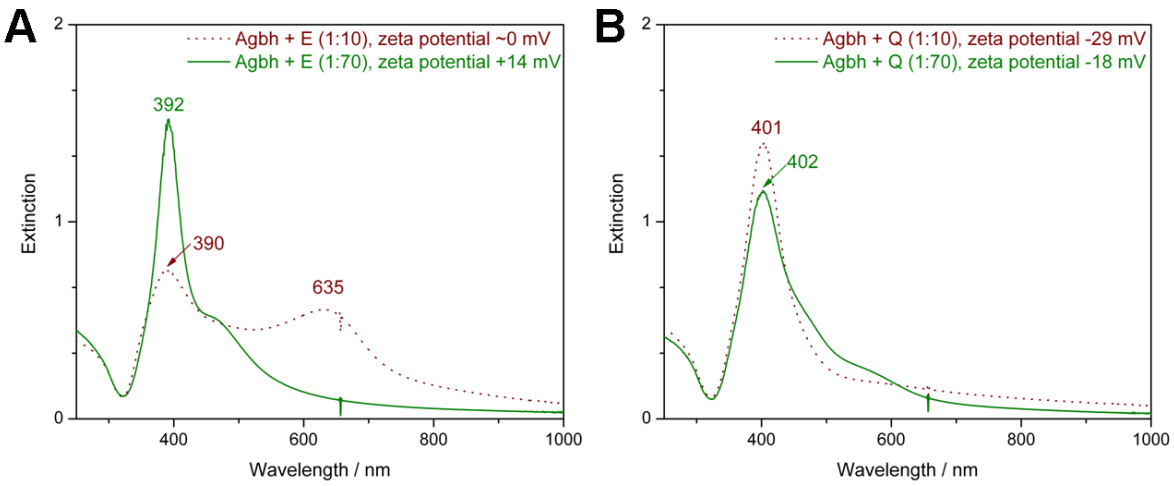

Figure 6. UV-Vis spectra of Agbh with the addition of (A) glutamic acid and/or (B) glutamine. Zeta potential values are also mentioned in graphs legend.

Lower concentration of E in Agbh+E (1:10) system induced an aggregation of AgNPs as can be derived from the appearance of a second maximum located at around 635 nm in the extinction spectrum of this system (Figure 6A, wine dotted curve). On the contrary, the higher E concentration (Agbh+E, 1:70) did not change dramatically the position of SPE band maximum and led only to the occurrence of a shoulder at approx. 460 nm (Figure 6A, olive solid curve). Simultaneously, zeta potential value of the parent Agbh colloid (−38 mV) was changed by the lower and higher E concentrations to 0 mV and +14 mV, respectively. These zeta potential values point to a complete (0 mV) and/or partial (+14 mV) destabilization of the systems (i.e., aggregation) which is consistent with the UV-Vis spectra presented in Figure 6A. DLS measurements also corroborated the more pronounced aggregation in Agbh+E (1:10) system by the mean size values of AgNPs being around 1070 nm; whereas approximately 64 nm in Agbh+E (1:70) only.

When glutamine added into Agbh in the mutual molar ratio of 1:10 (Ag:Q), it did not cause a dramatic change in the UV-Vis spectrum (Figure 6B, wine dotted curve) as that observed in the case of glutamic acid (in the same ratio toward Ag). Zeta potential value remained also quite negative

(−29 mV) and mean size of AgNPs determined by DLS reached approximately 30 nm; both values reporting about the stability of the system. On the other hand, increasing the Q concentration in the final Agbh+Q system (Ag:Q molar ratio of 1:70) resulted in a broadening of SPE band and appearance of a shoulder at around 580 nm (Figure 6B, olive solid curve). Zeta potential value decreased to −18 mV and DLS mean size augmented to ~ 359 nm.

In order to learn how each of the two amino acids interacts with the surface of AgNPs of Agbh colloid, surface-enhanced Raman scattering (SERS) and infrared (IR) absorption spectroscopies were used (Figure 7). For the former technique, the excitation wavelength of 633 nm was chosen with respect to the broadening of SPE band toward the infrared region and the appearance of the second maximum in the UV-Vis spectra presented in Figure 6. As previously explained, the broadening and occurrence of the second maximum are induced by the aggregation of AgNPs caused by the introduction of amino acids into Agbh colloidal solution. Therefore, information about the interaction of a particular amino acid with AgNPs has to be sought by using the excitation wavelength that matches the secondary maximum and/or shoulder. Then, the same excitation wavelength has to be used for all systems in order to compare them mutually and exclude any changes in spectra caused by molecular resonance. Of course, the absolute SERS spectral intensities (Figure 7A–B) can differ based on the extent of resonance with the excitation wavelength for a particular system. For instance, Agbh+E (1:10) is in the best resonance with 633 nm excitation laser beam, providing thus the best SERS signal (compare Figure 7A and B).

While SERS spectra revealed very similar relative intensities (within a particular SERS spectrum) and positions of peaks in both cases, Agbh+E as well as Agbh+Q (Figure 7A–B); IR absorption spectra of these systems differed significantly (Figure 7C–D). This discrepancy between the spectra stemming from two vibrational techniques can be easily explained by different selection rules being obeyed for the observation of vibration bands and different physical phenomenon being exploited in each of the two techniques.

The most intensive peak in SERS spectra was located at 241 ± 3 cm^{-1} (Figure 7A and 6B). It can be attributed to Ag-N covalent bond according to the literature [52]. The peak is, especially at less aggregated systems, broadened by a shoulder positioned at lower Raman shifts values, around 230 cm^{-1}. This can be most probably assigned to Ag-OOC bond [53,54]. The other peaks in SERS spectra (Figure 7A–B) can be assigned to borates and polyborates (e.g. 1390 cm^{-1}, stemming from the oxidation of borohydride during Agbh preparation), nitrate anion (e.g. 1045 cm^{-1}, coming from $AgNO_3$—the starting chemical for Agbh preparation), valence and deformation vibrations of amino acids (e.g. C-C, C-C-C, C-C-H, O-C-O, C-N-H etc. bonds) [52].

IR absorption spectra (Figure 7C and 7D) confirmed the presence of O-H, N-H, aliphatic C-H stretching and deformation bands [52,55]. The characteristic IR absorption peaks of a non-dissociated carboxylic acid positioned at ~ 1730 cm^{-1} and of a dissociated form (two bands at ~ 1600 and ~ 1400 cm^{-1}) were also detected in many cases (Figure 7C–D) pointing thus to the bonding of amino acids by their carboxylic groups to AgNPs surface [52]. The peak at 1670 cm^{-1}, attributed to NH_2-CO-R vibrational band of glutamine [52,55], increased in its intensity when going from the smaller to the higher ratio of Q:Ag (i.e., from 10:1 to 70:1) which is fully understandable (Figure 7D).

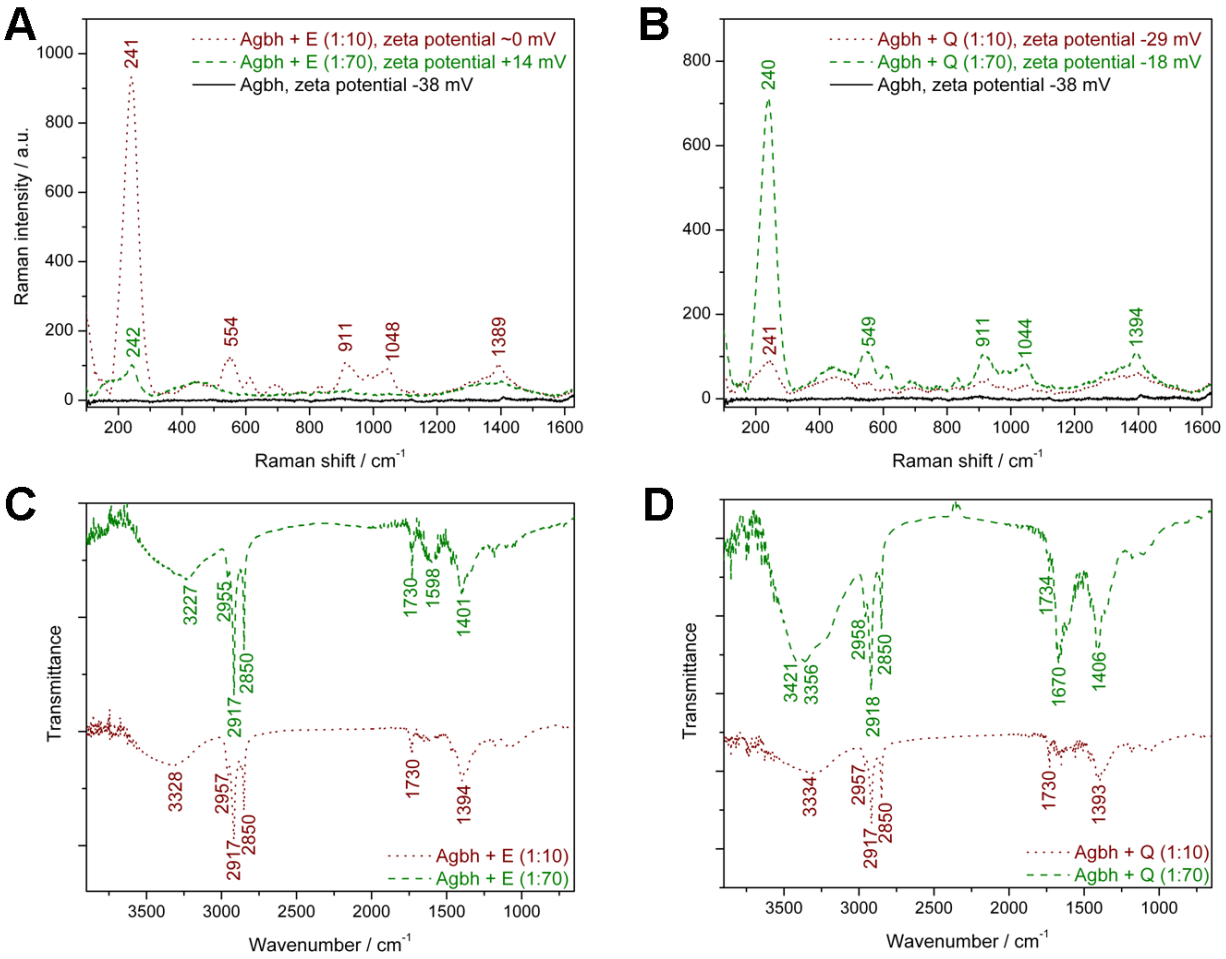

Figure 7. SERS spectra (A, B)—excitation wavelength 633 nm—and IR absorption spectra (C, D) of Agbh+E (A, C) and/or Agbh+Q (B, D) systems of both molar ratios investigated (Ag:AA of 1:10 and 1:70) are shown. Wine (dotted) and olive (dashed) colors (types) of the curves for the lower and the higher AA concentrations, respectively, are held. Only the most intensive and/or important peaks are labeled.

It can be thus summarized that both amino acids are bonded to AgNPs surface through covalent bonds and according to the concentration of a particular amino acid either Ag-N, or Ag-OOC bonds are dominant. This together with borates and their counter ions (Na^+) strongly influence the final zeta potential value of each system and consequently the AgNPs aggregation state.

MIC values determined for all four Agbh+AA systems (Figure 4) revealed pretty much the same values as those determined for the parent Agbh in the cases of both Gram-positive bacteria included in our study and Pseudomonas aeruginosa. The only difference in MIC value was systematically observed for Klebsiella pneumoniae, a lower MIC value for Agbh than for the other systems with amino acids. These results thus show rather no influence of different zeta potential values of engineered AgNPs (induced by AgNPs surface modification using the two selected amino acids of two different concentrations) on their antimicrobial properties. This can be understood as an indirect proof of the fact that the main toxicity of AgNPs is caused by dissolved Ag^+ ions rather than AgNPs themselves under the conditions of our antibacterial testing although the exact quantification of silver

ratio being present in the form of AgNPs vs Ag^+ [56] is not experimentally achievable nowadays.

4. Conclusion

The present work demonstrated that AgNPs are spontaneously formed from Ag^+ ions (introduced as $AgNO_3$) in M-H Broth under the conditions of microbes cultivation, without and/or with the presence of a microbe. The effect of glutamic acid and/or glutamine on the properties of spontaneously and engineered AgNPs was investigated as well. Due to surface-enhanced Raman scattering and IR absorption spectroscopies, covalent bonding of amino acids to AgNPs surface was evidenced. Characteristic features of AgNPs were changed upon the addition of both selected amino acids, however, the antibacterial activity remained almost unchanged. Antibacterial tests repeatedly revealed a higher toxicity of $AgNO_3$ (lower MIC values) in comparison to engineered AgNPs, although AgNPs were present in both systems. This can serve as an indirect proof of Ag^+ ions being the main source of AgNPs antibacterial activity.

Acknowledgments

K. M. S. thanks to the Grant Agency of the Czech Republic for financial support (grant no. P108 / 11 / P657). The authors gratefully acknowledge the support by the project LO1305 of the Ministry of Education, Youth and Sports of the Czech Republic and grant project LF_2013_012. Professors Virender K. Sharma from Texas A&M University, Radek Zboril from RCPTM and Rajender S. Varma from U.S. Environmental Protection Agency are thanked for their comments. The authors acknowledge also to three unknown referees for their time spent reviewing the manuscript and for their valuable comments.

Conflict of Interest

All authors declare no conflicts of interest in this paper.

References

1. Liu HH., Cohen Y (2014) Multimedia environmental distribution of engineered nanomaterials. *Environ Sci Technol* 48: 3281-3292.
2. Lopez-Serrano A, Olivas RM, Landaluze JS, et al. (2014) Nanoparticles: a global vision. Characterization, separation, and quantification methods. Potential environmental and health impact. *Anal Methods* 6: 38-56.
3. Li DW, Zhai WL, Li YT, Long YT (2014) Recent progress in surface enhanced Raman spectroscopy for the detection of environmental pollutants. *Microchim Acta* 181: 23-43.
4. Lalley J, Dionysiou DD, Varma RS, et al. (2014) Silver-based antibacterial surfaces for drinking water disinfection – an overview. *Curr Opin Chem Eng* 3: 25-29.
5. Han Ch, Likodimos V, Khan JA, et al. (2014) UV-visible Light-activated Ag-decorated, monodispersed TiO2 aggregates for treatment of the pharmaceutical oxytetracycline. *Environ Sci Pollut Res* 21: 11781-11793.

6. Windler I, Height M, Nowack B (2013) Comparative evaluation of antimicrobials for textile applications. *Environ Int* 53: 62-73.
7. Geranio L, Heuberger M, Nowack B (2009) The behavior of silver nanotextiles during washing. *Environ Sci Technol* 43: 8113-8.
8. Adegboyega NF, Sharma VK, Siskova K, et al. (2013) Interactions of Aqueous Ag^+ with Fulvic Acids: Mechanisms of Silver Nanoparticle Formation and Investigation of Stability. *Environ Sci Technol* 47: 757-764.
9. Akaighe N, MacCuspie RI, Navarro DA, et al. (2011) Humic acid-induced silver nanoparticle formation under environmentally relevant conditions. *Environ Sci Technol* 45: 3895-3901.
10. Nadagouda MN, Iyanna N, Lalley J, et al. (2014) Synthesis of silver and gold nanoparticles using antioxidants from blackberry, blueberry, pomegranate, and turmeric extracts. *ACS Sustanaible Chem Eng* 2: 1717-1723.
11. Markova Z, Siskova KM, Filip J, et al. (2013) Air stable magnetic bimetallic Fe-Ag nanoparticles for advanced antimicrobial treatment and phosphorus removal. *Environ Sci Technol* 47: 5285-5293.
12. Sigma-Aldrich. Inc., Product Information, 70192 Mueller Hinton Broth (M-H Broth). Available from: http://www.sigmaaldrich.com/content/dam/sigma-aldrich/docs/Fluka/Datasheet/70192dat.pdf
13. Sintubin L, Verstraete W, Boon N (2012) Biologically produced nanosilver: current state and future perspectives. *Biotechnol Bioeng* 109: 2422-2436.
14. Faramarzi MA, Sadighi A (2013) Insights into biogenic and chemical production of inorganic nanomaterials and nanostructures. *Adv Colloid Interface Sci* 189-190: 1-20.
15. Suman TY, Radhika Rajasree SR, Kanchana A, et al. (2013) Biosynthesis, characterization and cytotoxic effect of plant mediated silver nanoparticles using Morinda citrifolia root extract. *Colloids Surf B* 106: 74-78.
16. Kharissova OV, Dias HVR, Kharisov BI, et al. (2013) The greener synthesis of nanoparticles. *Trends Biotechnol* 31: 240-248.
17. Hu B, Wang SB, Wang K, et al. (2008) Microwave-assisted rapid facile "green" synthesis of uniform silver nanoparticles: self-assembly into multilayered films and their optical properties. *J Phys Chem C* 112: 11169-11174.
18. Alvarez-Puebla RA, Aroca RF (2009) Synthesis of silver nanoparticles with controllable surface charge and their application to surface-enhanced Raman scattering. *Anal Chem* 81: 2280-2295.
19. Khan Z, Talib A (2010) Growth of different morphologies (quantum dots to nanorod) of Ag-nanoparticles: role of cysteine concentration. *Coll Surf B* 76: 164-169.
20. Rafey A, Shrivastavaa KBL, Iqbal SA, et al. (2011) Growth of Ag-nanoparticles using aspartic acid in aqueous solutions. *J Colloid Interface Sci* 354: 190-195.
21. Jacob JA, Naumov S, Mukherjee T, et al. (2011) Preparation, characterization, surface modification and redox reactions of silver nanoparticles in the presence of tryptophan. *Coll Surf B* 87: 498-504.
22. Sondi I, Goia DV, Matijevic E (2003) Preparation of highly concentrated stable dispersions of uniform silver nanoparticles. J Colloid Interface Sci 260: 75-81.
23. Nadagouda MN, Varma RS (2008) Green synthesis of Ag and Pd nanospheres, nanowires, and nanorods using vitamin B2: catalytic polymerisation of aniline and pyrrole. *J Nanomat* 2008: 1-8.

24. Tan S, Erol M, Attygalle A, et al. (2007) Synthesis of positively charged silver nanoparticles via photoreduction of $AgNO_3$ in branched polyethyleneimine/HEPES solutions. *Langmuir* 23: 9836-9843.
25. Frattini A, Pellegri N, Nicastro D, et al. (2005) Effect of amine groups in the synthesis of Ag nanoparticles using aminosilanes. *Mater Chem Phys* 94: 148-152.
26. Xie J, Lee JY, Wang DIC, et al. (2007) Silver nanoplates: from biological to biomimetic synthesis. *ACS Nano* 1: 429-439.
27. Stevanovic M, Savanovic I, Uskokovic V, et al. (2012) A new, simple, green, and one-pot four-component synthesis of bare and poly(alpha,gamma, L-glutamic acid)-capped silver nanoparticles. *Colloid Polym Sci* 190: 221-231.
28. Yu DG (2007) Formation of colloidal silver nanoparticles stabilized by Na^+-poly(gamma-glutamic acid)-silver nitrate complex via chemical reduction process. *Coll Surf B* 59: 171-178.
29. Vigneshwaran N, Nachane RP, Balasubramanya RH (2006) A novel one-pot "green" synthesis of stable silver nanoparticles using soluble starch. *Carbohydr Res* 341: 2012-2018.
30. Raveendran P, Fu J, Wallen SL (2003) Completely "green" synthesis and stabilization of metal nanoparticles. *J Am Chem Soc* 125: 13940-13941.
31. Tai C, Wang YH, Liu HS (2008) A green process for preparing silver nanoparticles using spinning disk reactor. *AIChE J* 54: 445-452.
32. Sun SK, Wang HF, Yan XP (2011) A sensitive and selective resonance light scattering bioassay for homocysteine in biological fluids based on target-involved assembly of polyethyleneimine-capped Ag-nanoclusters. *Chem Commun* 47: 3817-3819.
33. Lee KJ, Browning LM, Nallathamby PD, et al. (2013) Study of charge-dependent transport and toxicity of peptide-functionalized silver nanoparticles using zebrafish embryos and single nanoparticle plasmonic spectroscopy. *Chem Res Toxicol* 26: 904-917.
34. Chernousova S, Epple M (2013) Silver as antibacterial agent: ion, nanoparticle, and metal. *Angew Chem Ind Ed* 52: 1636-1653.
35. Sharma VK, Siskova KM, Zboril R, et al. (2014) Organic-coated silver nanoparticles in biological and environmental conditions: Fate, stability and toxicity. *Adv Colloid Interface Sci* 204: 15-34.
36. Rai MK, Deshmukh SD, Ingle AP, et al. (2012) Silver nanoparticles: the powerful nanoweapon against multidrug-resistant bacteria. *J Appl Microbiol* 112: 841-852.
37. Li WR, Xie XB, Shi QS, et al. (2010) Antibacterial activity and mechanism of silver nanoparticles on Escherichia coli. *Appl Microbiol Biotechnol* 85: 1115-1122.
38. Li WR, Xie XB, Shi QS, et al. (2011) Antibacterial effect of silver nanoparticles on Staphylococcus aureus. *Biometals* 24: 135-141.
39. Lara HH, Ayala-Nunez NV, Turrent LCI, et al. (2010) Bactericidal effect of silver nanoparticles against multidrug-resistant bacteria. *World J Microbiol Biotechnol* 26: 615-621.
40. Lok CN, Ho CM, Chen R, et. al. (2006) Proteomic analysis of the mode of antibacterial action of silver nanoparticles. *J Proteome Res* 5: 916-924.
41. Yang XY, Gondikas AP, Marinakos SM, et al. (2012) Mechanism of silver nanoparticle toxicity is dependent on dissolved silver and surface coating in Caenorhabditis elegans. *Environ Sci Technol* 46: 1119−1127.

42. Morones JR, Elechiguerra, JL, Camacho A, et al. (2005) The bactericidal effect of silver nanoparticles. *Nanotechnology* 16: 2346.
43. Sondi I, Salopek-Sondi B (2004) Silver nanoparticles as antimicrobial agent: a case study on E. coli as a model for gram-negative bacteria. *J Colloid Interface Sci* 275: 177-182.
44. Xu H, Qu F, Xu H, et al. (2012) Role of reactive oxygen species in the antibacterial mechanism of silver nanoparticles on Escherichia coli O157:H7. *Biometals* 25: 45-53.
45. Choi O, Hu Z (2008) Size dependent and reactive oxygen species related nanosilver toxicity to nitrifying bacteria. *Environ Sci Technol* 42: 4583-4588.
46. Xiu ZM, Zhang QB, Puppala HL, et al. (2012) Negligible particle-specific antibacterial activity of silver nanoparticles. *Nano Lett* 12: 4271-4275.
47. El Badawy AM, Luxton TP, Silva RG, et al. (2010) Impact of environmental conditions (pH, ionic strength, and electrolyte type) on the surface charge and aggregation of silver nanoparticles suspensions. *Environ Sci Technol* 44: 1260-1266.
48. Siskova KM, Machala L, Tucek J, et al. (2013) Mixtures of L-amino acids as reaction medium for iron nanoparticles formation: the order of addition into ferrous salt solution matters. *Int J Mol Sci* 14: 19452-19473.
49. Sloufova I, Siskova K, Vlckova B, et al. (2008) SERS-activating effect of chlorides on borate-stabilized silver nanoparticles: formation of new reduced adsorption sites and induced nanoparticle fusion. *Phys Chem Chem Phys* 10: 2233-2242.
50. Siskova K, Becicka O, Safarova K, et al. (2013) HCl effect on two types of Ag nanoparticles utilizable in detection of low concentrations of organic species. *Sustainable nanotechnology and the environment: advances and achievements* 1124: 151-163.
51. Sriramulu DD, Lunsdorf H, Lam JS, et al. (2005) Microcolony formation: a novel biofilm model of Pseudomonas aeruginosa for the cystic fibrosis lung. *J Med Microbiol* 54: 667-676.
52. Nakamoto K (2009) Infrared and Raman spectra of inorganic and coordination compounds, part B, Hoboken, New Jersey, USA, John Wiley & Sons, Inc., 26-84 and 388-392.
53. Moskovits M, Suh JS (1985) Confirmation of mono- and dicarboxylic acids adsorbed on silver surfaces. *J Am Chem Soc* 107: 6826-6829.
54. Munro CH, Smith WE, Garner M, et al. (1995) Characterization of the surface of a citrate-reduced colloid optimized for use as a substrate for surface-enhanced resonance Raman scattering. *Langmuir* 11: 3712-3720.
55. Lindon JC (2000) Encyclopedia of spectroscopy and spectrometry, part II, San Diego, Academic press, 1035-1057.
56. Schaumann GE, Philippe A, Bundschuh M, et al. (2014) Understanding the fate and biological effects of Ag- and TiO_2- nanoparticles in the environment: The quest for advanced analytics and interdisciplinary concepts. *Sci Total Environ:* S0048-9697: 1473-1479.

AIMS Press